

Kinetic Theory of Granular Shear Flow: Constitutive Relations for the Hard-Disk Model

Sang Rak Kim¹ and Leslie V. Woodcock²

Received April 14, 1992; final September 14, 1992

A kinetic theory for the constitutive rheological relations of rapid granular shear flow of hard circular disks, characterized by a coefficient of restitution e and a surface roughness coefficient β , is formulated. From a set of general constitutive equations for single-particle dynamical variables, the approximate expressions for the limit of small and large dimensionless dissipative parameter R_t are obtained. Here R_t is defined as the ratio $\sigma\gamma/\langle v \rangle$, where v is the fluctuation of translational velocity from the mean flow velocity, σ is the diameter of a disk, and γ is the shear rate. At small R_t the theoretical predictions can be compared with "exact" computer simulation results of granular dynamics that are also reported. The agreement between theory and simulation is better than expected; the present theory is accurate up to high packing density in this region of R_t .

KEY WORDS: Kinetic theory; granular flow; constitutive relations.

1. INTRODUCTION

A granule is a small, hard, compact, solid particle that is an aggregate of molecules via strong intermolecular forces. A granular material is a collection of a large number of discrete granules. When the local stress is small, a granular material behaves like an elastic solid so that it may support an external load. The maximum load is limited insofar as the frictional bonds between granular particles can support it. When the magnitudes of local stresses exceed this limit, the granular particles can begin to flow. The initial flow involves many-particle blocks moving together relative to one another along shear bands. If the motion occurs slowly, the particles will

¹ Physics Department, Kyonggi University, Suwon, 440-760, Korea.

² Department of Chemical Engineering, University of Bradford, Bradford BD7 1DP, West Yorkshire, U.K.

stay in contact and interact frictionally in neighboring blocks. This is the quasistatic regime of granular flow.

If the magnitudes of local stresses are sufficiently large so that each granular particle can move freely and independently of each other, instead of aggregate blocks, this flow regime is called grain-inertia. In the present paper we report a kinetic theory approach to this rapid flow regime, initially in two dimensions. Previous theoretical and simulation studies of rapid granular flow are described in the review articles of Savage⁽¹⁾ and Campbell.⁽²⁾

In this rapid-flow regime, the velocity \mathbf{v} of each particle can be decomposed into a sum of the mean velocity \mathbf{u} of the bulk material and a random component \mathbf{V} to describe the motion of particles relative to the mean. The translational "granular temperature" T_t may be defined by^(1,2)

$$2T_t = \langle \mathbf{V}^2 \rangle \quad (1)$$

where $\mathbf{V} = \mathbf{v} - \mathbf{u}$ and is the instantaneous deviation from the mean velocity $\mathbf{u} = \langle \mathbf{v} \rangle$. The angular brackets denote the usual ensemble average of particle space and time.

To describe theoretically the rapid-flow behavior of an idealized frictional hard-sphere model granular material, it is natural to exploit the similarity to the problem of transport between the molecules of a gas and the granular particles. Since collisions between granular particles are dissipative through inelasticity and surface friction, standard kinetic theory for dense gases must be extended to accommodate this aspect of the physics. The earliest such theoretical approach was applied to a dense system of identical, smooth, slightly inelastic spheres.⁽³⁾ This approach has been extended to rough, slightly inelastic spheres⁽⁴⁾ by taking into consideration the rotational spin degrees of freedom of granular particles.

In the present approach, we begin in two dimensions, for two reasons. First, the physics of rotational motion and the effects of interparticle friction are conceptually easier to understand and more easily treated with less damage to the physical properties by the approximations involved. Second, the theoretical predictions can be tested in computer simulations of a large number of disks in a plane more economically, and with more insight, than in 3D.^(5,6) There is no evidence from these previous simulations to suggest any significantly new physical concept between two- and three-dimensional rapid granular flow.

To treat collisions between granular particles, it is assumed that they are binary and instantaneous and that the velocities of a pair of colliding particles are distributed at random, and that there is no correlation between the velocity and the coordinate of a particle, i.e., the molecular

chaos assumption.⁽⁷⁾ The single-particle velocity distribution function, in a simple shearing flow, is assumed to be a local Maxwellian distribution, involving two granular temperatures T_t and T_r : T_t measures the mean kinetic energy of fluctuations in the translational velocity, and T_r measures the mean kinetic energy of fluctuations in the spin angular velocity. The pair correlation function at contact should reflect the anisotropy induced in the system by the shear flow. With these assumptions accurate constitutive relations can be derived for strongly dissipative systems besides nearly conserved systems akin to molecular gas theory models.

In the next section, transport equations for mass, linear momentum, spin angular momentum, translational kinetic energy, and spin angular kinetic energy for simple shear flow are derived. The constitutive relations between stresses and the rate of shear strain are subsequently derived for both the weakly and strongly dissipative regimes. In Section 3 new computer simulation results are presented for granular dynamics of the idealized frictional hard-disk model and compared with the kinetic theory predictions.

2. KINETIC THEORY

Let us consider a granular system of identical circular rigid disks, each having a mass m , a diameter σ , and a moment of inertia I about an axis through the center of mass perpendicular to the disk itself, moving in a plane y - z under a simple shear flow with a shear rate $\gamma = \partial u_y / \partial z$, where u_y is a local flow velocity along the y direction. The disks also spin about axes perpendicular to the plane through their centers, so $\boldsymbol{\omega} = \omega \hat{x}$, where \hat{x} is a unit vector along the x axis. Let us denote $\Psi(\mathbf{r}, t)$ as a single-particle dynamical variable at position \mathbf{r} and time t . The ensemble average of $\Psi(\mathbf{r}, t)$ is written as

$$\langle \Psi(\mathbf{r}, t) \rangle = \frac{1}{n(\mathbf{r}, t)} \int d\mathbf{v} d\boldsymbol{\omega} \Psi(\mathbf{r}, t) f^{(1)}(\mathbf{r}, \mathbf{v}, \boldsymbol{\omega}; t) \quad (2)$$

where $n(\mathbf{r}, t) = \int d\mathbf{v} d\boldsymbol{\omega} f^{(1)}(\mathbf{r}, \mathbf{v}, \boldsymbol{\omega}; t)$, the number density distribution function at position \mathbf{r} and time t , and the single-particle distribution function $f^{(1)}(\mathbf{r}, \mathbf{v}, \boldsymbol{\omega}; t)$ is defined such that $f^{(1)}(\mathbf{r}, \mathbf{v}, \boldsymbol{\omega}; t) \delta\mathbf{v} \delta\boldsymbol{\omega}$ is the number of particles per unit volume around \mathbf{r} with translational velocities within the range \mathbf{v} and $\mathbf{v} + \delta\mathbf{v}$ and with spin angular velocities within the range $\boldsymbol{\omega}$ and $\boldsymbol{\omega} + \delta\boldsymbol{\omega}$. The balance equation for the change of $\langle n\Psi \rangle$ is

$$\frac{\partial}{\partial t} \langle n\Psi \rangle = n \langle D\Psi \rangle - \nabla \cdot \langle n\mathbf{v}\Psi(\mathbf{r}, t) \rangle - \nabla \cdot \boldsymbol{\Theta} + \chi \quad (3)$$

where

$$\langle D\Psi \rangle = \left\langle \frac{\partial \Psi}{\partial t} \right\rangle + \left\langle \mathbf{v} \cdot \frac{\partial \Psi}{\partial \mathbf{r}} \right\rangle + \left\langle \mathbf{f}^b \cdot \frac{\partial \Psi}{\partial \mathbf{v}} \right\rangle \quad (4)$$

and \mathbf{f}^b is the body force per unit mass. The first term is due to the fact that the quantity for each particle changes intrinsically. The second term is due to the net flux of particles which enter the volume element in time dt . The third involves a collisional transfer term

$$\begin{aligned} \Theta = & -\frac{\sigma^2}{2} \int_{\mathbf{v}_{12} \cdot \hat{k} > 0} d\hat{k} d\mathbf{v}_1 d\mathbf{v}_2 d\boldsymbol{\omega}_1 d\boldsymbol{\omega}_2 (\Psi'_1 - \Psi_1)(\mathbf{v}_{12} \cdot \hat{k}) \hat{k} \\ & \times f^{(2)} \left(\mathbf{r} - \frac{1}{2} \sigma \hat{k}, \mathbf{v}_1, \boldsymbol{\omega}_1; \mathbf{r} + \frac{1}{2} \sigma \hat{k}, \mathbf{v}_2, \boldsymbol{\omega}_2; t \right) \end{aligned} \quad (5)$$

and the last term involves a collisional source-like effect

$$\begin{aligned} \chi = & \frac{\sigma}{2} \int_{\mathbf{v}_{12} \cdot \hat{k} > 0} d\hat{k} d\mathbf{v}_1 d\mathbf{v}_2 d\boldsymbol{\omega}_1 d\boldsymbol{\omega}_2 (\Psi'_2 + \Psi'_1 - \Psi_2 - \Psi_1)(\mathbf{v}_{12} \cdot \hat{k}) \\ & \times f^{(2)} \left(\mathbf{r} - \frac{1}{2} \sigma \hat{k}, \mathbf{v}_1, \boldsymbol{\omega}_1; \mathbf{r} + \frac{1}{2} \sigma \hat{k}, \mathbf{v}_2, \boldsymbol{\omega}_2; t \right) \end{aligned} \quad (6)$$

where $\mathbf{v}_{12} = \mathbf{v}_1 - \mathbf{v}_2$ and \hat{k} is a unit vector along the line of centers from particle 1 to particle 2 at contact.

The integration should be done over the collision condition $\mathbf{v}_{12} \cdot \hat{k} > 0$. And the two-particle distribution function $f^{(2)}(\mathbf{r}_1, \mathbf{v}_1, \boldsymbol{\omega}_1; \mathbf{r}_2, \mathbf{v}_2, \boldsymbol{\omega}_2; t)$ is defined such that

$$f^{(2)}(\mathbf{r}_1, \mathbf{v}_1, \boldsymbol{\omega}_1; \mathbf{r}_2, \mathbf{v}_2, \boldsymbol{\omega}_2; t) \delta \mathbf{r}_1 \delta \mathbf{r}_2 \delta \mathbf{v}_1 \delta \mathbf{v}_2 \delta \boldsymbol{\omega}_1 \delta \boldsymbol{\omega}_2$$

is the probability of finding a pair of particles 1 and 2 in the volume element $\delta \mathbf{r}_1, \delta \mathbf{r}_2$ centered on the points $\mathbf{r}_1, \mathbf{r}_2$ and having translational velocities within the ranges \mathbf{v}_1 and $\mathbf{v}_1 + \delta \mathbf{v}_1, \mathbf{v}_2$ and $\mathbf{v}_2 + \delta \mathbf{v}_2$ and spin angular velocities within the ranges $\boldsymbol{\omega}_1$ and $\boldsymbol{\omega}_1 + \delta \boldsymbol{\omega}_1, \boldsymbol{\omega}_2$ and $\boldsymbol{\omega}_2 + \delta \boldsymbol{\omega}_2$, respectively. Now if we take a single-particle property Ψ as mass m , linear momentum $m\mathbf{v}$, spin angular momentum $I\boldsymbol{\omega}$, translational kinetic energy $\frac{1}{2}m\mathbf{v}^2$, and spin rotational kinetic energy $\frac{1}{2}I\boldsymbol{\omega}^2$, respectively, we get a set of transport equations describing the balance laws of each dynamical variable:

$$\frac{d\rho}{dt} = -\rho \nabla \cdot \mathbf{u} \quad (7)$$

$$\rho \frac{d\mathbf{u}}{dt} = \rho \mathbf{f}^b - \nabla \cdot \mathbf{P} \quad (8)$$

$$nI \frac{d\boldsymbol{\omega}_0}{dt} = -\nabla \cdot \mathbf{N} + \chi(I\boldsymbol{\omega}) \quad (9)$$

$$\rho \frac{dT_t}{dt} = \mathbf{P} : \nabla \mathbf{u} - \nabla \cdot \mathbf{Q}_t - \chi_t \quad (10)$$

$$\frac{1}{2} \rho \frac{dT_r}{dt} = -\mathbf{N} : \nabla \boldsymbol{\omega}_0 - \nabla \cdot \mathbf{Q}_r - \boldsymbol{\omega}_0 \cdot \chi(I\boldsymbol{\omega}) - \chi_r \quad (11)$$

where $\rho = mn$, the bulk mass density; $\boldsymbol{\omega}_0 = \langle \boldsymbol{\omega} \rangle$, the mean spin angular velocity; and $\frac{1}{2}mT_r = \frac{1}{2}I\langle \mathbf{W}^2 \rangle$, the spin angular fluctuation kinetic energy, where $\mathbf{W} = \boldsymbol{\omega} - \boldsymbol{\omega}_0$.

The pressure tensor \mathbf{P} , the spin angular momentum \mathbf{N} , the translational energy flux \mathbf{Q}_t , and the spin rotational energy flux \mathbf{Q}_r may be each divided into two parts, a kinetic part and a configurational part, denoted by subscripts k and c , respectively.

$$\mathbf{P}_k = \rho \langle \mathbf{V}\mathbf{V} \rangle \quad (12)$$

$$\mathbf{P}_c = \Theta(m\mathbf{V}) \quad (13)$$

$$\mathbf{N}_k = nI \langle \mathbf{V}\mathbf{W} \rangle \quad (14)$$

$$\mathbf{N}_c = \Theta(I\mathbf{W}) \quad (15)$$

$$\mathbf{Q}_{tk} = \frac{1}{2}\rho \langle \mathbf{V}\mathbf{V}^2 \rangle \quad (16)$$

$$\mathbf{Q}_{tc} = \Theta(\frac{1}{2}m\mathbf{V}^2) \quad (17)$$

$$\mathbf{Q}_{rk} = \frac{1}{2}nI \langle \mathbf{V}\mathbf{W}^2 \rangle \quad (18)$$

$$\mathbf{Q}_{rc} = \Theta(\frac{1}{2}I\mathbf{W}^2) \quad (19)$$

Furthermore, the rate of translational kinetic energy interchange per unit volume is defined as

$$\chi_t = -\chi(\frac{1}{2}m\mathbf{V}^2) \quad (20)$$

and the rate of spin rotational kinetic energy interchange per unit volume as

$$\chi_r = -\chi(\frac{1}{2}I\mathbf{W}^2) \quad (21)$$

In the present case, during a collision between granular particles, kinetic energies may be dissipated through inelasticity and also through

surface roughness and an exchange between translational and spin rotational kinetic energy may occur through surface roughness. Due to imperfect frictional slip there is, in fact, an incomplete equipartition of the translational and spin rotational kinetic energies so that there exist two kinds of granular temperatures T_t and T_r .

We now approximate the single-particle distribution function under simple shear flow by a local Maxwellian of the form involving two temperatures T_t and T_r ,

$$f^{(1)}(\mathbf{r}, \mathbf{v}, \boldsymbol{\omega}; t) \cong \frac{n(\mathbf{r}, t)}{(2\pi T_t)(2\pi m T_r/I)^{1/2}} \exp\left(-\frac{(\mathbf{v}-\mathbf{u})^2}{2T_t}\right) \times \exp\left(-\frac{I(\boldsymbol{\omega}-\boldsymbol{\omega}_0)^2}{2mT_r}\right) \quad (22)$$

with $\mathbf{u} = \mathbf{u}(\mathbf{r}, t) = \mathbf{u}(z) \hat{y}$, where \hat{y} is the unit vector along the y axis.

Next, assuming instantaneous binary collision and the molecular chaos assumption, we can approximate the two-particle distribution function at contact simply by

$$f^{(2)}(\mathbf{r} - \frac{1}{2}\sigma\hat{k}, \mathbf{v}_1, \boldsymbol{\omega}_1; \mathbf{r} + \frac{1}{2}\sigma\hat{k}, \mathbf{v}_2, \boldsymbol{\omega}_2; t) \cong g(\mathbf{r} - \frac{1}{2}\sigma\hat{k}, \mathbf{r} + \frac{1}{2}\sigma\hat{k}; t) f^{(1)}(\mathbf{r} - \frac{1}{2}\sigma\hat{k}, \mathbf{v}_1, \boldsymbol{\omega}_1; t) f^{(1)}(\mathbf{r} + \frac{1}{2}\sigma\hat{k}, \mathbf{v}_2, \boldsymbol{\omega}_2; t) \quad (23)$$

If we integrate Eq. (23) with respect to translational velocities $\mathbf{v}_1, \mathbf{v}_2$ and spin angular velocities $\boldsymbol{\omega}_1, \boldsymbol{\omega}_2$, we get, assuming the system to be homogeneous and steady,

$$\int d\mathbf{v}_1 d\mathbf{v}_2 d\boldsymbol{\omega}_1 d\boldsymbol{\omega}_2 f^{(2)}(\mathbf{r} - \frac{1}{2}\sigma\hat{k}, \mathbf{v}_1, \boldsymbol{\omega}_1; \mathbf{r} + \frac{1}{2}\sigma\hat{k}, \mathbf{v}_2, \boldsymbol{\omega}_2; t) = n^2 g(\sigma\hat{k}; v) \quad (24)$$

Furthermore, we also get, in equilibrium at contact,

$$2 \int_{\mathbf{v}_{12} \cdot \hat{k} > 0} d\mathbf{v}_1 d\mathbf{v}_2 d\boldsymbol{\omega}_1 d\boldsymbol{\omega}_2 f^{(2)}(\mathbf{r} - \frac{1}{2}\sigma\hat{k}, \mathbf{v}_1, \boldsymbol{\omega}_1; \mathbf{r} + \frac{1}{2}\sigma\hat{k}, \mathbf{v}_2, \boldsymbol{\omega}_2; t) = n^2 g_0(\sigma; v) \quad (25)$$

where $g_0(\sigma, v)$ is the equilibrium radial distribution function at contact and v is a volume fraction.

If we combine Eqs. (22)–(25), we get a first-order approximation to the anisotropic radial distribution at contact,

$$\begin{aligned}
 g\left(\mathbf{r}-\frac{1}{2}\sigma\hat{\mathbf{k}}, \mathbf{r}+\frac{1}{2}\sigma\hat{\mathbf{k}}; t\right) &= g(\sigma\hat{\mathbf{k}}; v) \\
 &\cong (2/n^2) \int_{\mathbf{v}_{12}\cdot\hat{\mathbf{k}}>0} d\mathbf{v}_1 d\mathbf{v}_2 d\boldsymbol{\omega}_1 d\boldsymbol{\omega}_2 g_0(\sigma; v) f^{(1)}\left(\mathbf{r}-\frac{1}{2}\sigma\hat{\mathbf{k}}, \mathbf{v}, \boldsymbol{\omega}; t\right) \\
 &\quad \times f^{(1)}\left(\mathbf{r}+\frac{1}{2}\sigma\hat{\mathbf{k}}, \mathbf{v}, \boldsymbol{\omega}; t\right) \\
 &= g_0(\sigma, v) \operatorname{erfc}\left(\frac{\hat{\mathbf{k}}\cdot[\mathbf{u}(\mathbf{r}-\frac{1}{2}\sigma\hat{\mathbf{k}})-\mathbf{u}(\mathbf{r}+\frac{1}{2}\sigma\hat{\mathbf{k}})]}{2(T_t)^{1/2}}\right) \\
 &= g_0(\sigma, v) \operatorname{erfc}\left\{-\left[\frac{1}{2(2)^{1/2}}\right] R_t \sin 2\theta\right\} \tag{26}
 \end{aligned}$$

where $\operatorname{erfc}(z)$ is the complementary error function defined by

$$\operatorname{erfc}(z) = 1 - \operatorname{erf}(z) = \frac{2}{\pi^{1/2}} \int_z^\infty dt \exp(-t^2) \tag{27}$$

and the dimensionless parameter R_t is defined by

$$R_t = \sigma\gamma / \langle \mathbf{V}^2 \rangle^{1/2} \tag{28}$$

and θ is defined as the angle between the y axis and $\hat{\mathbf{k}}$.

Now we should consider a collisional model between two rough, inelastic circular identical hard particles 1 and 2, each having a diameter σ , and having translational velocities \mathbf{v}_1 and \mathbf{v}_2 , and spin angular velocities $\boldsymbol{\omega}_1$ and $\boldsymbol{\omega}_2$, respectively. The total relative velocity at the contact point just prior to the collision is

$$\mathbf{g}_{12} = \mathbf{v}_{12} - \frac{1}{2}\sigma\hat{\mathbf{k}} \times \boldsymbol{\Omega} \tag{29}$$

where $\boldsymbol{\Omega} = \boldsymbol{\omega}_1 + \boldsymbol{\omega}_2$. During a collision between granular particles the components of \mathbf{g}_{12} are changed such that

$$\hat{\mathbf{k}} \cdot \mathbf{g}'_{12} = -e(\hat{\mathbf{k}} \cdot \mathbf{g}_{12}) \tag{30}$$

$$\hat{\mathbf{k}} \times \mathbf{g}'_{12} = -\beta(\hat{\mathbf{k}} \times \mathbf{g}_{12}) \tag{31}$$

where the primed quantities denote values after the collision. In fact, the coefficient of restitution e and the coefficient of surface roughness β are defined by Eqs. (30) and (31).

Using Eqs. (29)–(31), we get the relationships between the pre- and postcollisional velocities,

$$\mathbf{v}'_1 - \mathbf{v}_1 = -\eta_2 \mathbf{v}_{12} - (\eta_1 - \eta_2) \hat{k}(\hat{k} \cdot \mathbf{v}_{12}) + \eta_2 \frac{1}{2} \sigma \hat{k} \times \boldsymbol{\Omega} \quad (32)$$

$$\mathbf{v}'_2 - \mathbf{v}_2 = -(\mathbf{v}'_1 - \mathbf{v}_1) \quad (33)$$

and

$$\boldsymbol{\omega}'_1 - \boldsymbol{\omega}_1 = -\eta_2 \frac{m\sigma}{2I} (\hat{k} \times \mathbf{v}_{12}) - \eta_2 K^{-1} \boldsymbol{\Omega} \quad (34)$$

$$\boldsymbol{\omega}'_2 - \boldsymbol{\omega}_2 = \boldsymbol{\omega}'_1 - \boldsymbol{\omega}_1 \quad (35)$$

where

$$\eta_1 = \frac{1+e}{2}$$

$$\eta_2 = \frac{1+\beta}{2} \frac{K}{1+K}$$

and K is the radius of gyration of a disk along the axis perpendicular to the y - z plane,

$$K = \frac{4I}{m\sigma^2}$$

The change of translational kinetic energy during a collision is expressed as

$$\begin{aligned} \Delta(\text{TKE}) &= \frac{1}{2} m [(\mathbf{v}'_1)^2 + (\mathbf{v}'_2)^2 - \mathbf{v}_1^2 - \mathbf{v}_2^2] \\ &= -\eta_2 (1 - \eta_2) m \mathbf{v}_{12}^2 - [(\eta_1 - \eta_2)(1 - \eta_1 - \eta_2)] m (\hat{k} \cdot \mathbf{v}_{12})^2 \\ &\quad + \eta_2 (1 - 2\eta_2) \frac{1}{2} m \sigma \hat{k} \times \boldsymbol{\Omega} \cdot \mathbf{v}_{12} + \eta_2^2 K^{-1} I [\boldsymbol{\Omega}^2 - (\hat{k} \cdot \boldsymbol{\Omega})^2] \quad (36) \end{aligned}$$

and the change of spin angular kinetic energy during a collision is

$$\begin{aligned} \Delta(\text{RKE}) &= \frac{1}{2} I [(\boldsymbol{\omega}'_1)^2 + (\boldsymbol{\omega}'_2)^2 - \boldsymbol{\omega}_1^2 - \boldsymbol{\omega}_2^2] \\ &= \eta_2 \left\{ \left(\frac{m}{K} \right) \eta_2 (\hat{k} \times \mathbf{v}_{12})^2 + \frac{1}{2} m \sigma \left(\frac{2\eta_2}{K} - 1 \right) (\hat{k} \times \mathbf{v}_{12} \cdot \boldsymbol{\Omega}) \right. \\ &\quad \left. + \frac{I}{K} \left(\frac{\eta_2}{K} - 1 \right) \boldsymbol{\Omega}^2 \right\} \quad (37) \end{aligned}$$

Note that no dissipation is involved to damp the random motions when $e = 0$ or 1 and $\beta = -1$, in which cases $\Delta(\text{TKE}) = \Delta(\text{RKE}) = 0$ identically, irrespective of its initial states.

From Eqs. (5), (13), (22), (23), and (32), we can calculate the configurational pressure tensor,

$$\begin{aligned}
 \mathbf{P}_c &= \Theta(m\mathbf{V}) \\
 &= -\frac{1}{2}\sigma^2 \int_{\mathbf{v}_{12} \cdot \hat{k} > 0} m \left[-\eta_2 \mathbf{v}_{12} - (\eta_1 - \eta_2) \hat{k} (\hat{k} \cdot \mathbf{v}_{12}) + \eta_2 \frac{1}{2} \sigma \hat{k} \times \boldsymbol{\Omega} \right] \\
 &\quad \times \hat{k} (\mathbf{v}_{12} \cdot \hat{k}) g(\sigma \hat{k}; v) f^{(1)} \left(\mathbf{r} - \frac{1}{2} \sigma \hat{k}, \mathbf{v}_1, \boldsymbol{\omega}_1 \right) f^{(1)} \left(\mathbf{r} + \frac{1}{2} \sigma \hat{k}, \mathbf{v}_2, \boldsymbol{\omega}_2 \right) \\
 &\quad \times d\hat{k} d\mathbf{v}_1 d\mathbf{v}_2 d\boldsymbol{\omega}_1 d\boldsymbol{\omega}_2 \\
 &= \frac{\sigma^2}{2\pi} m n^2 g_0 T_t \int_0^{2\pi} d\theta \operatorname{erfc} \left(-\frac{R_t}{2\sqrt{2}} \sin 2\theta \right) \left\{ (2\pi)^{1/2} \eta_2 R_t (2 \sin^2 \theta - 1) \hat{n} \hat{k} \right. \\
 &\quad \times \left[\frac{1}{2} \exp \left(-\frac{1}{8} R_t^2 \sin^2 2\theta \right) + \frac{1}{4} \left(\frac{\pi}{2} \right)^{1/2} R_t \sin 2\theta \operatorname{erfc} \left(-\frac{R_t}{2\sqrt{2}} \sin 2\theta \right) \right] \\
 &\quad + \sqrt{\pi \eta_1} \hat{k} \hat{k} \frac{R_t}{\sqrt{2}} \sin 2\theta \exp \left(-\frac{1}{8} R_t^2 \sin^2 2\theta + \sqrt{\pi} R_t^2 \sin^2 2\theta + 1 \right) \\
 &\quad \left. \times \operatorname{erfc} \left(-\frac{R_t}{2\sqrt{2}} \sin 2\theta \right) \right\} \quad (38)
 \end{aligned}$$

where \hat{n} is a unit vector normal to \hat{k} .

From Eqs. (6), (22), (23), and (34), we can also calculate

$$\begin{aligned}
 \chi(I\boldsymbol{\omega}) &= \frac{\sigma}{2} \int_{\mathbf{v}_{12} \cdot \hat{k} > 0} I(\boldsymbol{\omega}'_1 + \boldsymbol{\omega}'_2 - \boldsymbol{\omega}_1 - \boldsymbol{\omega}_2) (\hat{k} \cdot \mathbf{v}_{12}) g(\sigma \hat{k}; v) \\
 &\quad \times f^{(1)} \left(\mathbf{r} - \frac{1}{2} \sigma \hat{k}, \mathbf{v}_1, \boldsymbol{\omega}_1 \right) f^{(1)} \left(\mathbf{r} + \frac{1}{2} \sigma \hat{k}, \mathbf{v}_2, \boldsymbol{\omega}_2 \right) d\hat{k} d\mathbf{v}_1 d\mathbf{v}_2 d\boldsymbol{\omega}_1 d\boldsymbol{\omega}_2 \\
 &= -\frac{1}{2\sqrt{\pi}} \eta_2 m \sigma^2 n^2 g_0(\sigma; v) \\
 &\quad \times \int_0^{2\pi} d\theta \left(-\sigma \gamma \sin^2 \theta + \sigma \omega_0 \right) \operatorname{erfc} \left(-\frac{R_t}{2\sqrt{2}} \sin 2\theta \right) \\
 &\quad \times \left[\frac{1}{2} \exp \left(-\frac{1}{8} R_t^2 \sin^2 2\theta \right) + \frac{\pi}{4\sqrt{2}} R_t \sin 2\theta \operatorname{erfc} \left(-\frac{R_t}{2\sqrt{2}} \sin 2\theta \right) \right] \quad (39)
 \end{aligned}$$

From Eqs. (6), (20), (22), (23), and (36), we get

$$\begin{aligned}
 \chi_t &= -\frac{\sigma}{2} \int_{\mathbf{v}_{12} \cdot \hat{k} > 0} \frac{1}{2} m [(\mathbf{v}'_1)^2 + (\mathbf{v}'_2)^2 - \mathbf{v}_1^2 - \mathbf{v}_2^2] (\hat{k} \cdot \mathbf{v}_{12}) \\
 &\quad \times g(\sigma \hat{k}; \nu) f^{(1)}\left(\mathbf{r} - \frac{1}{2} \sigma \hat{k}, \mathbf{v}_1, \boldsymbol{\omega}_1\right) \\
 &\quad \times f^{(1)}\left(\mathbf{r} + \frac{1}{2} \sigma \hat{k}, \mathbf{v}_2, \boldsymbol{\omega}_2\right) d\hat{k} d\mathbf{v}_1 d\mathbf{v}_2 d\boldsymbol{\omega}_1 d\boldsymbol{\omega}_2 \\
 &= -\frac{\sigma}{2} m n^2 g_0(\sigma; \nu) T_t (T_t/4\pi)^{1/2} \\
 &\quad \times \int_0^{2\pi} d\theta \operatorname{erfc}\left(-\frac{R_t}{2\sqrt{2}} \sin 2\theta\right) \left\{ 16\eta_1(\eta_1 - 1) \right. \\
 &\quad \times \left[\frac{1}{2} \left(\frac{1}{8} R_t^2 \sin^2 2\theta + 1 \right) \exp\left(-\frac{1}{8} R_t^2 \sin^2 2\theta\right) + \frac{1}{2} \left(\frac{\pi}{2}\right)^{1/2} \sin 2\theta \right] \\
 &\quad \times \left[\frac{1}{16} \left(R_t^2 \sin^2 2\theta + \frac{3}{4} \right) \operatorname{erfc}\left(-\frac{1}{2\sqrt{2}} \sin 2\theta\right) \right] \\
 &\quad + \left[2\eta_2(\eta_2 - 1)(R_t^2 \sin^4 \theta + 1) \right. \\
 &\quad + \sqrt{2} \eta_2(1 - 2\eta_2) \frac{\sigma \omega_0}{\sqrt{T_t}} (R_t \sin^2 \theta) + \eta_2^2 \left(\frac{(\sigma \omega_0)^2}{T_t} + \frac{2T_r}{KT_t} \right) \left. \right] \\
 &\quad \times \left[2 \exp\left(-\frac{1}{8} R_t^2 \sin^2 2\theta\right) \right. \\
 &\quad \left. \left. + \frac{\sqrt{\pi}}{\sqrt{2}} R_t \sin 2\theta \operatorname{erfc}\left(-\frac{1}{2\sqrt{2}} R_t \sin 2\theta\right) \right] \right\} \quad (40)
 \end{aligned}$$

Finally, from Eqs. (6), (21)–(23), and (37),

$$\begin{aligned}
 \chi_r &= -\frac{\sigma}{2} \int_{\mathbf{v}_{12} \cdot \hat{k} > 0} \frac{1}{2} m [(\boldsymbol{\omega}'_1)^2 + (\boldsymbol{\omega}'_2)^2 - \boldsymbol{\omega}_1^2 - \boldsymbol{\omega}_2^2] (\hat{k} \cdot \mathbf{v}_{12}) \\
 &\quad \times g(\sigma \hat{k}; \nu) f^{(1)}\left(\mathbf{r} - \frac{1}{2} \sigma \hat{k}, \mathbf{v}_1, \boldsymbol{\omega}_1\right) \\
 &\quad \times f^{(1)}\left(\mathbf{r} + \frac{1}{2} \sigma \hat{k}, \mathbf{v}_2, \boldsymbol{\omega}_2\right) d\hat{k} d\mathbf{v}_1 d\mathbf{v}_2 d\boldsymbol{\omega}_1 d\boldsymbol{\omega}_2
 \end{aligned}$$

$$\begin{aligned}
&= -\frac{\sigma}{2} mn^2 g_0(\sigma; \nu) T_t \left(\frac{4T_t}{\pi}\right)^{1/2} \int_0^{2\pi} d\theta \operatorname{erfc}\left(-\frac{R_t}{2\sqrt{2}} \sin 2\theta\right) \\
&\quad \times \left[\frac{1}{2} \exp\left(-\frac{1}{8} R_t^2 \sin^2 2\theta\right) \right. \\
&\quad \left. + \frac{1}{4} \left(\frac{\pi}{2}\right)^{1/2} R_t \sin 2\theta \operatorname{erfc}\left(-\frac{1}{2\sqrt{2}} R_t \sin 2\theta\right)\right] \\
&\quad \times \left[\frac{2}{K} \eta_2^2 (R_t^2 \sin^4 \theta + 1) - 2\eta_2 \left(\frac{2}{K} - 1\right) \frac{\sigma\omega_0}{\sqrt{T_t}} R_t \sin^2 \theta \right. \\
&\quad \left. + \eta_2 \left(\frac{\eta_2}{K} - 1\right) \left(\frac{(\sigma\omega_0)^2}{T_t} + 2\frac{T_r}{KT_t}\right)\right] \quad (41)
\end{aligned}$$

The dimensionless parameter R_t , already defined in Eq. (28), is the ratio between the characteristic mean flow velocity difference due to applied shear rate γ and the root-mean-square value of the granular particle translational fluctuation velocity from the mean. If there exists a small energy dissipation in the system, for example, with nearly elastic particles involved, then R_t becomes small compared to 1. On the contrary, if there exists a large energy dissipation in the system, for example, with nearly inelastic particles involved or in a colloidal system where the interstitial fluid is very dense and viscous, R_t becomes large compared to 1. In a system with large R_t , given shear rate γ , a translational fluctuation velocity acquired from a collision returns quickly to its mean flow velocity.

If we expand Eq. (38) to third order in R_t , we get the symmetric stress tensor;

$$\begin{aligned}
P_c &= \frac{\sigma^2}{2\pi} mn^2 g_0 T_t \left[\pi^2 \eta_1 (\hat{y}\hat{y} + \hat{z}\hat{z}) - R_t \left(\frac{\pi}{2}\right)^{3/2} (2\eta_1 + \eta_2) (\hat{y}\hat{z} + \hat{z}\hat{y}) \right. \\
&\quad \left. + R_t^2 \left(\pi + \frac{1}{2}\right) \frac{\pi}{2} \eta_1 (\hat{y}\hat{y} + \hat{z}\hat{z}) \right. \\
&\quad \left. - R_t^3 \left(\frac{23\pi(1 + \sqrt{2}) - 3\pi}{8\sqrt{(2\pi)}} \eta_1 + \frac{3}{4\sqrt{(2\pi)}} \eta_2\right) \frac{1}{8} \pi (\hat{y}\hat{z} + \hat{z}\hat{y}) \right] \quad (42)
\end{aligned}$$

Also, from Eqs. (39)–(41), we get, to second order in R_t ,

$$\chi(I\omega) = -\frac{1}{2\sqrt{\pi}} \eta_2 mn^2 \sigma^3 g_0 \left[\pi + R_t^2 \left(\frac{\sqrt{\pi}}{8} - \frac{1}{16}\right) \pi \right] (2\omega_0 - \gamma) \quad (43)$$

$$\begin{aligned}
\chi_t = & -\frac{\sigma}{2} mn^2 g_0 \frac{T_t^2}{\sqrt{4\pi T_t}} \left\{ 2\pi \left[8\eta_1(\eta_1 - 1) + 4\eta_2(\eta_2 - 1) + \frac{4}{K} \eta_2^2 \frac{T_r}{T_t} \right] \right. \\
& + R_t^2 \left[3\eta_1(\eta_1 - 1)\pi + 6\pi\eta_2(\eta_2 - 1) - 4\pi \sqrt{2}\eta_2(1 - 2\eta_2) \frac{\sigma\omega_0}{R_t \sqrt{T_t}} \right. \\
& \left. \left. + 4\pi\eta_2^2 \left(\frac{\sigma\omega_0}{\sqrt{T_t}} \right)^2 + \frac{1}{2} \frac{\pi T_r}{KT_t} \right] \right\} \quad (44)
\end{aligned}$$

$$\begin{aligned}
\chi_r = & -\sigma mn^2 g_0 \frac{T_t^2}{\sqrt{4\pi T_t}} \left(2\pi \left[\frac{2}{K} \eta_2^2 + \eta_2 \left(\frac{\eta_2}{K} - 1 \right) \frac{2T_r}{KT_t} \right] \right. \\
& + R_t^2 \left\{ \frac{3\pi}{2K} \eta_2^2 - 2\eta_2 \left(\frac{2}{K} - 1 \right) \pi \frac{\sigma\omega_0}{R_t \sqrt{T_t}} \right. \\
& + \eta_2 \left(\frac{\eta_2}{K} - 1 \right) 2\pi \left(\frac{\sigma\omega_0}{R_t \sqrt{T_t}} \right)^2 + \frac{\pi}{4} \left[\frac{2}{K} \eta_2^2 + \eta_2 \left(\frac{\eta_2}{K} - 1 \right) \frac{2T_r}{KT_t} \right] \\
& \left. \left. + \frac{\pi}{8} \left[\frac{2}{K} \eta_2^2 + \eta_2 \left(\frac{\eta_2}{K} - 1 \right) \frac{2T_r}{KT_t} \right] \right\} \right) \quad (45)
\end{aligned}$$

Assuming a steady and uniform bulk system, as in Eq. (24), we find that the mean spin angular velocity equation (9), translational kinetic energy equation (10), and rotational kinetic equation (11) are reduced to

$$\chi(I\omega) = 0 \quad (46)$$

$$\gamma \mathbf{P}_{zy} + \chi_t = 0 \quad (47)$$

$$\chi_r = 0 \quad (48)$$

Equation (46) is the conservation of the rate of spin angular momentum transfer; Eq. (47) is a balance law between the shear work and the rate of translational kinetic energy interchange. External shear work should be supplied to maintain the translational and rotational velocity fluctuations. Equation (48) tells us that the rate of spin rotational kinetic energy interchange is zero.

If we insert Eq. (39) into (46), we get the general expression

$$\omega_0 = \frac{1}{2}\gamma \quad (49)$$

Thus, the mean spin angular velocity ω_0 should always be equal to half of the shear rate γ applied to the bulk system, independent of the magnitude of R_t .

Now, if we consider Eqs. (42), (44), and (45) to first order in R_t and insert Eqs. (47) and (48), we get

$$\frac{T_r}{T_t} = \frac{\eta_2}{1 - \eta_2 K^{-1}} \quad (50)$$

$$R_t = 2 \left(\frac{2\eta_1(1 - \eta_1) + \eta_2(1 - \eta_2) - \eta_2^3(K - \eta_2)}{2\eta_1 + \eta_2} \right)^{1/2} \quad (51)$$

Equations (49) and (50) are the same as in the 3D case, but the expression for R_t in Eq. (51) shows only a small difference.⁽²⁾

From Eq. (42), we get

$$S = \left| \frac{P_{yz}}{P_{yy}} \right| = \frac{3\eta_1 + \eta_2}{2\sqrt{(2\pi)\eta_1}} R_t \quad (52)$$

Now let us turn to the other extreme, i.e., the large- R_t solution. From Eq. (38), we get, in the limit $R_t \rightarrow \infty$, the symmetric stress tensor,

$$P_c = \frac{\pi}{2} mn^2 \sigma^2 g_0 R_t^2 T_t \left[\eta_1 (\hat{y}\hat{y} + \hat{z}\hat{z}) - \left(\frac{8}{3\pi} \eta_1 + \frac{1}{3\pi} \eta_2 \right) (\hat{y}\hat{z} + \hat{z}\hat{y}) \right] \quad (53)$$

This expression tells us that the normal stress and the shear stress are proportional to the square of the shear rate, which is the same as Bagnold's experiment⁽⁵⁾ on wax spheres suspended in a glycerine-water-alcohol mixture and sheared in a coaxial cylindrical rheometer. The ratio of normal stress to shear stress S is

$$S = \frac{(8/3\pi)\eta_1 + (1/3\pi)\eta_2}{\eta_1} \quad (54)$$

From Eq. (40), we get in the limit $R_t \rightarrow \infty$,

$$\begin{aligned} \chi_t = & -mn^2 \sigma g_0 \frac{T_t^2}{\sqrt{\pi} T_t} R_t \left[\frac{3}{4} \left(\frac{\pi}{2} \right)^{1/2} - \eta_1(\eta_1 - 1) R_t^2 + \frac{4}{3} \eta_2(\eta_2 - 1) \right. \\ & \left. + 2\eta_2(1 - 2\eta_2) \frac{R_t^2}{\sqrt{2}} + 2\eta_2^2 \left(\frac{R_t^2}{2} + \frac{2T_r}{KT_t} \right) \right] \quad (55) \end{aligned}$$

Also, from Eq. (41),

$$\chi_r = \sqrt{2} \sigma m n^2 g_0 T_i^{3/2} R_i \left[\eta_2 \left(\frac{2}{K} - 1 \right) \frac{1}{\sqrt{2}} R_i^2 - \frac{2}{3} K^{-1} \eta_2^2 R_i^2 + \eta_2 (1 - K^{-1} \eta_2) \left(\frac{1}{2} R_i^2 + 2K^{-1} \frac{T_i}{T_i} \right) \right] \quad (56)$$

3. COMPUTER SIMULATIONAL RESULTS

We considered N identical circular disks which are characterized by a coefficient of restitution e and a surface roughness coefficient β defined in Eqs. (30) and (31). The granular dynamics is quite similar in method to molecular dynamics. However, there is one great difference. In molecular dynamics, to simulate a shearing system, we need some special techniques such as the velocity rescaling to keep the system at constant temperature. On the contrary, there is no need of an artificial thermostat to maintain constant temperature of the system in granular dynamics. To see the bulk properties of the simple shear flow, we adopt the usual Lees-Edwards periodic boundary condition.⁽⁶⁾ The overlapping hard-sphere method was used to reduce the computer time. This was originally used for a hard-sphere potential with an attractive potential tail.⁽⁷⁾ All the particle positions are displaced during a fixed time interval. There exist inevitably overlapping pairs which should not be allowed due to the hardness of the granular particles. The overlapping of particle pairs should be resolved according to the rules of collision through Eqs. (32)–(35). In this way we can generate the positions and velocities of the particles. More details can be found in refs. 7 and 8.

We found that the properties of the nonequilibrium steady state are independent of the initial conditions of the granular dynamics. This steady state is attained after as few as 300 collisions per particle by the balance between the driving shear stress and the dissipative collisions through inelasticity and surface roughness. Also, as far as bulk properties are concerned, there are only slight changes in system properties when we take the number of granular particles N greater than 100. The averages are taken

Table I. Translational Granular Temperature T_i versus Shear Rate γ at $v=0.5$, $e=\beta=0.9$

| γ | 0.1 | 0.5 | 1.0 | 5.0 | 10.0 |
|----------|-------|------|------|-------|--------|
| T_i | 0.025 | 0.57 | 2.24 | 55.10 | 221.78 |

Table II. Translational Granular Temperature T_t versus Volume Fraction v at $\gamma = 0.5$, $e = \beta = 0.9$

| v | 0.2 | 0.3 | 0.4 | 0.5 | 0.6 | 0.7 |
|-------|------|------|------|------|------|------|
| T_t | 2.27 | 1.01 | 0.69 | 0.57 | 0.48 | 0.44 |

over a further 500 collisions per particle after the establishment of the steady state. The number of granular particles in our simulations is taken as $N = 200$. To express all the quantities in reduced units, the mass of a granular particle m , the diameter of a granular particle σ , and an appropriate acceleration constant a are taken as the corresponding units.

The simulational value of the mean spin angular velocity ω_0 is, of course, half of the shear rate γ , as predicted by Eq. (49). This attainment reflects one of the typical properties of the nonequilibrium steady state of a granular bulk system.

The granular temperatures are proportional to the square of the shear rate γ as shown in Table I. This is consistent with the granular temperature generation mechanism due to external shear stress.⁽⁹⁾ In Table II we show the granular temperature variation with respect to volume fraction v at fixed shear rate $\gamma = 0.5$ with $e = \beta = 0.9$. In Table III we also show the granular temperature variation with respect to the coefficient of restitution e . As expected, the granular temperature becomes small as the volume fraction v becomes large and the coefficient of restitution e small. This is consistent with our physical intuition. The configurational part of compressibility factor y is calculated by

$$y = \frac{PA}{NT_t} \quad (57)$$

where P is the trace of the pressure tensor \mathbf{P} , and A is a $2D$ volume. The configurational part of the stress is due to the transport of the linear momentum by interparticle collisions, at which the linear momentum is

Table III. Translational Granular Temperature T_t versus Coefficient of Restitution e at $v = \gamma = 0.5$, $\beta = 0.9$

| e | 0.95 | 0.90 | 0.85 | 0.80 | 0.75 |
|-------|------|------|------|------|------|
| T_t | 0.92 | 0.57 | 0.37 | 0.27 | 0.22 |

exchanged between the two colliding particles according to (32)–(35). The theoretical prediction is obtained from Eq. (42);

$$y = 2\eta_1 v g_0(\sigma; v) \quad (58)$$

Here we take g_0 as the 2D equivalent form of the Carnahan–Starling equation for the pair correlation function,⁽¹⁰⁾

$$g_0(\sigma; v) = \frac{1 + \frac{1}{8}v^2}{(1 - v)^2} \quad (59)$$

As shown in Fig. 1, there is an excellent agreement between the theoretical predictions and the simulational results. The ratio T_r/T_t is shown in Fig. 2 for both $K=0.5$ and $K=1.0$, together with the simulational results for $K=0.5$. When $\beta = -1.0$ from Eq. (34), T_r does not change from its initial value. However, near $\beta \sim -1.0$, $T_r/T_t \sim 0$ because there is a very small chance of transforming external shear work into rotational kinetic energy of the granular particle. In theory, as $\beta \rightarrow 1.0$, $T_r \sim T_t$ due to the equipartition of fluctuation kinetic energy between translational and spin rotational modes of motion. However, there is a significant discrepancy between the theoretical and simulational results. This is mainly due to the neglect of the

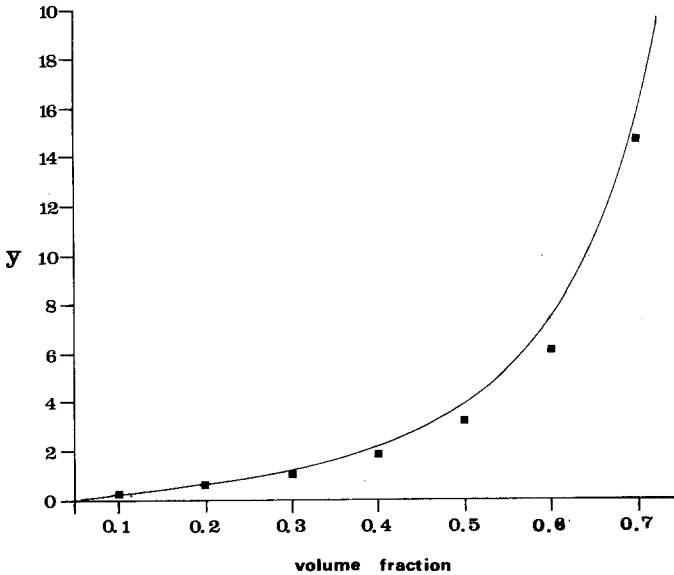


Fig. 1. Compressibility factor y versus volume fraction v at $\gamma=0.5$, $e=\beta=0.9$. The filled boxes represent the simulational data.

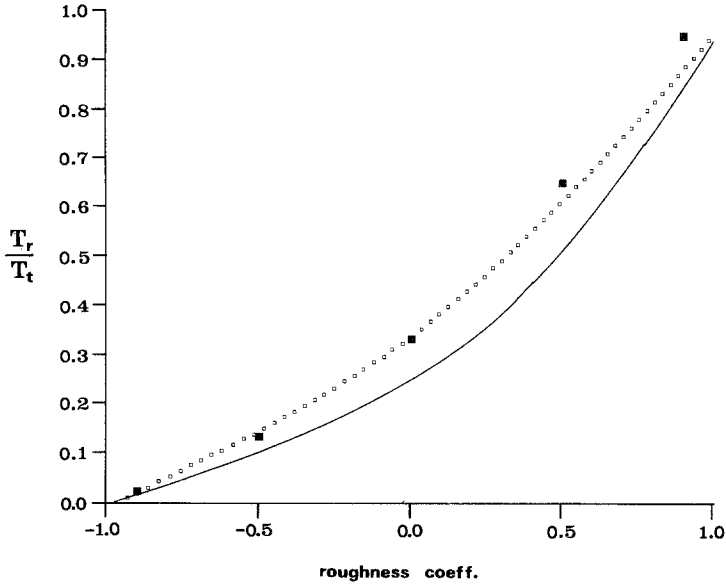


Fig. 2. Temperature ratio T_r/T_t versus coefficient of surface roughness β . (—) $K=0.5$, (□) $K=1.0$, (■) $K=0.5$, simulation.

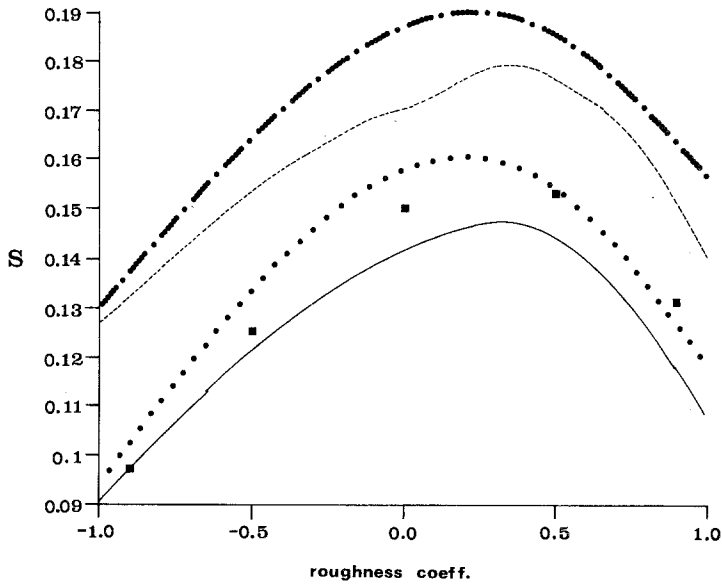


Fig. 3. Stress ratio S versus coefficient of surface roughness β . (—) $e=0.9$, $K=0.5$; (···) $e=0.9$, $K=1.0$; (---) $e=0.8$, $K=0.5$; (-·-) $e=0.8$, $K=1.0$; (■) $e=0.9$, $K=0.5$, simulation.

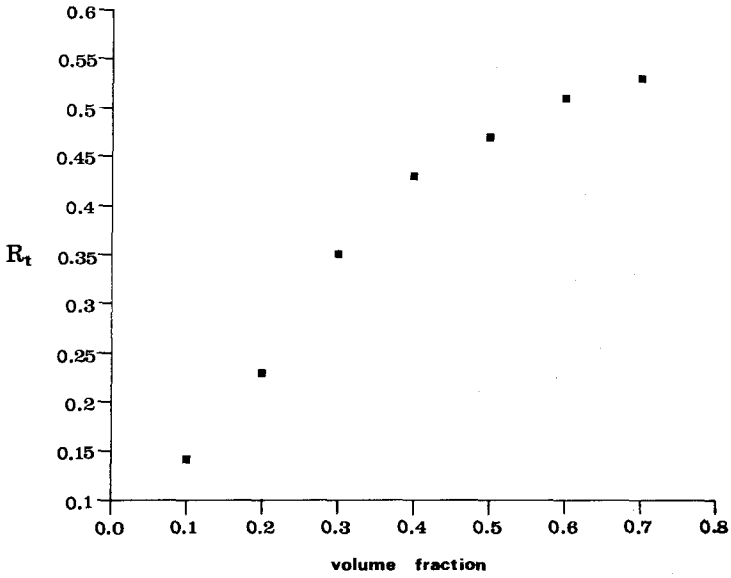


Fig. 4. Dimensionless parameter R_t versus volume fraction v , showing an asymptotic behavior at large v .

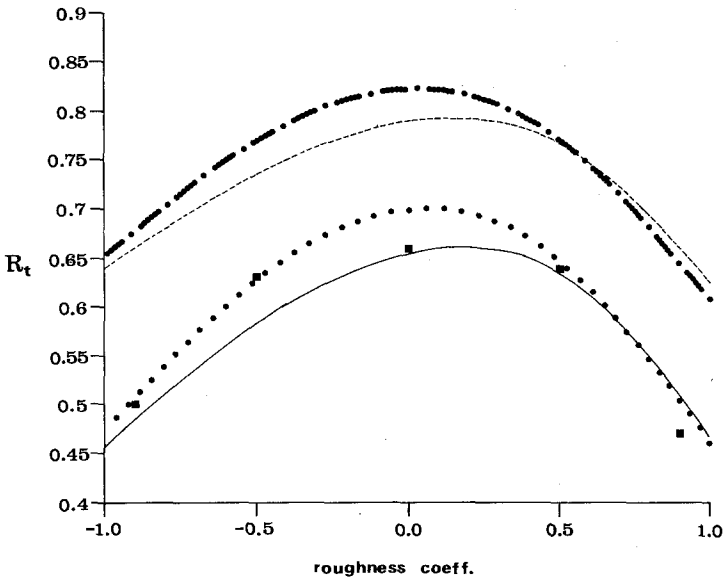


Fig. 5. Dimensionless parameter R_t versus coefficient of surface roughness β . (—) $e=0.9$, $K=0.5$; (...) $e=0.9$, $K=1.0$; (---) $e=0.8$, $K=0.5$; (- - -) $e=0.8$, $K=1.0$; (■) $e=0.9$, $K=0.5$, simulation.

second-order effect of R_t in Eq. (50). The disk with $K=1$ corresponds to a 2D ring, i.e., the masses are concentrated just on the perimeter. When K becomes large, there are more chances to have a large fluctuation of spin rotational velocity. The stress ratio S in Eq. (52) is shown in Fig. 3. We found that the simulated values are about 3–4 times larger than the theoretical values, but that, as shown in Fig. 3, if reduced to a factor of 3.2, the trends with respect to surface roughness coefficient β are quite similar. When K becomes large or e becomes smaller, S is increased accordingly. This is due to the fact that the tangential velocity change is larger compared to the normal velocity change as in Eq. (34).

The simulational dissipative parameter R_t , shown in Fig. 4, seems to have an asymptotic behavior as v increases. However, we could not extend the results to the further dense region due to the very short collision time and/or incomplete resolution of overlapping pairs. In fact, the maximum limit of the volume fraction at which the system can be sheared is around $v_m=0.79$ for two-dimensional monosized disks.

In Fig. 5 we show R_t with respect to β . The value of R_t becomes smaller at large $|\beta|$. The simulational values are quite similar to the theoretical values at low $|\beta|$, but a small discrepancy occurs at large $|\beta|$. The value of R_t becomes larger as e becomes smaller and K larger. One interesting result is that crossover occurs between the $K=0.5$ and $K=1.0$ cases near $\beta=0.5$. At large β , it takes a little more time to return to the mean translational velocity, as K becomes smaller. The simulational values of R_t are, unexpectedly, rather large even at $e=0.9$. The underlying assumption of the theoretical formulation is that R_t should be small compared to 1. However, the predictions of R_t are quite comparable with the simulational results.

4. CONCLUSION

We have derived general constitutive equations for a two-dimensional granular system under simple shear flow, from which we have obtained the expressions for the small- and large- R_t limits, respectively. We could not compare the values for the large- R_t limit with the simulational results, which could not be obtained at this point.

In the small- R_t limit, we compared the theoretical prediction with the simulational results. The granular temperatures with respect to the shear rate $\dot{\gamma}$ and volume fraction v are consistent with physical intuition. The simulated compressibility factor γ is quite comparable to the theoretical value. The mean spin angular velocity ω_0 is quite close to half of the shear strain rate $\dot{\gamma}$ as predicted. The ratio T_r/T_t is quite comparable at small $|\beta|$, but there are some discrepancies at large $|\beta|$. The simulated value for the

stress ratio S is about 3–4 times larger than the theoretical value, but the trends with respect to β are quite similar. The simulated value of R_i with respect to the volume fraction v shows an asymptotic behavior at large v . The simulational value of R_i is quite comparable to the theoretical result.

There still exist many discrepancies between simulational results and the theoretical results, which should be examined further. These discrepancies seem to be mainly due to the assumptions of a local Maxwellian velocity distribution and of molecular chaos.

ACKNOWLEDGMENTS

This work has been greatly supported by an SERC grant. One of us (S. R. K.) appreciates the partial support of KOSEF grant No. 91-8-00-05 and also the Research Center of Thermal and Statistical Physics of Korea University and the 1992 research subsidy of Kyoggi University.

REFERENCES

1. S. Savage, *Adv. Appl. Mech.* **24**:289 (1984).
2. C. Campbell, *Annu. Rev. Fluid Mech.* **22**:57 (1990).
3. C. Lun, S. Savage, D. Jeffrey, and N. Chepuruiy, *J. Fluid Mech.* **140**:223 (1984).
4. C. Lun and S. Savage, *ASME J. Appl. Mech.* **54**:47 (1987).
5. C. Campbell and C. Brennen, *J. Fluid Mech.* **151**:167 (1985).
6. C. Campbell and A. Gong, *J. Fluid Mech.* **164**:107 (1986).
7. D. McQuarrie, *Statistical Mechanics* (Harper and Row, New York, 1976).
8. R. Bagnolds, *Proc. R. Soc. Lond. A* **225**:49 (1954).
9. A. Lees and S. Edwards, *J. Phys. C: Solid State Phys.* **5**:1921 (1972).
10. S. Kim, *J. Korean Phys. Soc.* **23**:308 (1990).
11. M. Hopkins and M. Louge, *Phys. Fluids A* **3**:47 (1991).
12. N. Carnahan and K. Starling, *J. Chem. Phys.* **51**:635 (1969).
13. M. Turner and L. Woodcock, *Powder Tech.* **60**:47 (1990).